



On Characterizing Flow Resistance in a Tidal Reach

Ye Jing¹(✉), Xueting Lei², Jie Qin¹, Teng Wu¹,
and Elikplim Agbemafle¹

¹ College of Harbour, Coastal and Offshore Engineering, Hohai University,
Nanjing, China

liaozihu@qq.com, {jqin, wuteng}@hhu.edu.cn

² Changjiang Waterway Planning, Design and Research Institute, Wuhan, China

Abstract. The tidal reaches are characterized by unsteady and non-uniform flow (UNF), which is significantly different from the commonly assumed steady and uniform flow (SUF) in hydraulics. The SUF shows invariant temporal and spatial flow characteristics, and thus flow acceleration is absent in a prismatic channel. However, for the UNF, the variation of flow velocity and depth in both temporal and spatial scales causes the loss of flow energy, and thus increases the flow resistance. In order to clarify the variation of flow resistance and its influencing factors in tidal reaches, this study investigates the flow resistance characteristics under UNF conditions. In this study, a typical tidal section of the Lower Yangtze River (LYR) – Kouanzhi Waterway (KW) – was selected as the study area, where the temporal variation of water surface along the river course at different tide levels, the bathymetry of multiple cross-sections, the distribution of cross-sectional flow velocity and its temporal variation were measured in detail. Based on these field measurement data, the contribution terms to the energy slope were calculated and evaluated, by decomposing the momentum equation. The calculated contributing terms include water surface gradient, local acceleration, and convective acceleration. The results showed that the local acceleration and convective acceleration have a substantial impact on the energy slope during specific time periods, which was found to be more significant than the findings in previous studies. The results show that the local acceleration term is more significant than the convective acceleration term except when the water surface slope is close to zero, and its contribution is significant throughout the flood tide and the initial ebb tide periods. The above research results are of great significance for the investigation of flow resistance mechanisms and numerical simulations in tidal rivers.

Keywords: Momentum equation · Flow resistance · Energy slope · Tidal river

1 Introduction

Resistance coefficients of rivers vary with flow conditions and physical boundaries, such as bed roughness, cross-sectional geometry, river planar forms, the spatial distribution of roughness, and other factors that cause resistance changes (Yen 2002); Pagliara and Chiavaccini (2006) studied the hydraulics of rough channels with or

without the insertion of protruding boulders and influencing parameters such as slope, and relative submergence, and blocks disposition were systematically investigated. Rubol et al. (2018) explored the effect of canopy morphology on vegetated channel flow structure and resistance by treating the canopy as a porous medium characterized by an effective permeability. In addition to the roughness influence, Hohermuth and Weitbrecht (2018) found that bed-load transport significantly decreased flow resistance and increased near-bed velocity for the conditions investigated.

2 Literature

Most existing studies related to flow resistance assumed steady and uniform flow conditions, without considering the unsteadiness of flow. For steady flow in a prismatic channel, there is no temporal and spatial variation of flow velocity and flow depth, indicating no temporal and spatial gradient for velocity and depth. In contrast, the variation in the velocity and depth introduces extra loss of flow energy in comparison to steady and uniform flow, e.g., the flow processes in tidal rivers (Brown and Richard 1980). Specifically, there is a lack of knowledge and data to reliably estimate the flow resistance in tidal reaches which is a vital component in calibrating numerical models. Mrokowska et al. (2015) analyzed friction slope, friction velocity, and Manning coefficient in unsteady flow and they found that the former two parameters are more sensitive to applying simplified formulas than the Manning coefficient. Note that their measurements were obtained from artificial dam-break flood waves in a small lowland watercourse. Bao et al. (2018) investigated a modified formula aimed at improving the prediction of unsteady flow resistance. They proposed an equation including ten terms relating to the first- and second-order temporal and spatial partial derivatives of hydraulic parameters. Their results showed that the optimal number of additional terms is three, and extra terms can barely improve the unsteady friction estimation. These three items correspond to the three first-order derivatives in previous research (Rowiński et al. 2000; Mrokowska et al. 2015).

This study aims at analyzing the effect of unsteady flow characteristics on the energy slope in a large tidal river based on measured data and then compares the results with previous findings obtained from small channels. The method and data acquisition are given in Sect. 2, the results of the analysis are provided in Sect. 3, and this study is concluded in Sect. 5.

3 Methodology

For a one-dimensional channel, the momentum equation for unsteady flow is (Knight 1981):

$$-S_f = \frac{\partial \eta}{\partial x} + \frac{U}{g} \frac{\partial U}{\partial x} + \frac{1}{g} \frac{\partial U}{\partial t} + \frac{h + \eta}{2\rho} \frac{\partial \rho}{\partial x} \quad (1)$$

where η is the water level; U is the average cross-sectional flow velocity; x is the distance; t is the time; h is the depth; ρ is the fluid density, and g is the acceleration of gravity. With the help of the S_f , resistance coefficients can be calculated by resistance formulas, such as the Manning equation. The four terms on the right-hand side in Eq. (1) represent the slope of water surfaces, the convective acceleration, the local acceleration, and the density gradient, respectively. The last term is not considered in this study given the invariant flow density. For unsteady flow, the first three terms on the right-hand side determine the magnitude of the energy slope. Therefore, the main task of this study is to study the contribution of the three terms to the energy slope.

The KW is located in the LYR (latitude and longitude: 119°41'36.6", 32°15'6.1"). The Datong hydrological station, about 350 km upstream of the KW, is the last runoff observation station of the Yangtze River. This station has an annual average flow discharge of 28,700 m³/s and an annual average sediment concentration of 0.461 kg/m³. The KW is a tidal reach and its flow process is influenced by both runoff and tides. Normally, there is no reversing flow in the KW during the moderate flood and flood periods and occurs only during the spring tide in dry seasons. Therefore, the main driving force in the river section is the upstream runoff and is affected by the downstream tidal processes (Cao et al. 2011).

To study the resistance caused by the temporal and spatial variation of flow processes, the following data were collected: the temporal variation of water surface along the river course, the cross-sectional profiles along the river course, and the temporal cross-sectional distribution of flow velocity. These data were collected during spring tides in February 2019 (dry season) and May-June 2014 (flood season). The streamwise variation of the water surface was measured by temporary tidal stations, indicated by the solid red points in Fig. 1. The cross-section profiles and flow velocity were obtained by ADCP measurements indicated by the black solid lines. Due to the long distance among measured cross-sections, this study spatially interpolated the upstream and downstream cross-sections (red solid lines) near the measured cross-sections, and the convective acceleration terms are calculated based on these interpolated cross-sections and the accordant measured cross-sections. In addition, the interval of measured water level was 1 h, which was interpolated into an interval of 15 min. The water level was recorded relative to the 1956 Yellow Sea Height Datum of China. By spatially and temporally interpolating the measured data, the time series of water level along the course and the spatial distribution of cross-sectional flow velocity were obtained. Based on these data, the water level and flow velocity were spatially differenced to obtain the terms in Eq. (1).

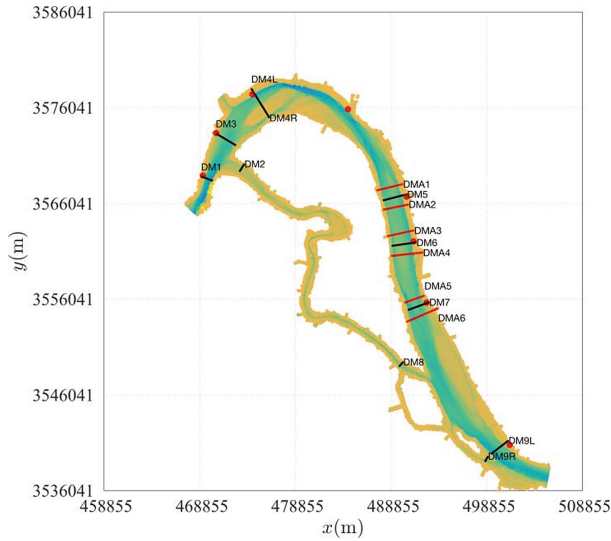


Fig. 1. Locations of water surface and ADCP measurements in the KW. The black and red cross-sections indicate the measured and interpolated locations, respectively.

4 Results

4.1 Variation of the Terms of Energy Slope in the Flood Season

Figure 2 shows the calculated results of the terms of the energy slope for the cross-sections DMA1 and DMA2 during a complete tidal cycle. The results of the other cross-sections are similar to those of the two sections. In each plot in Fig. 2, the upper subplot shows the temporal process of the contribution of each term in Eq. (1), and the lower subplot shows the corresponding temporal tide level (L_w) and depth-averaged velocity (U) process. The temporal variation of the components is similar in magnitude, in spite of the fact that more fluctuations occur in DMA2 because of the more evident temporal variation of the water surface gradient in this cross-section. The S_f continuously changes with the variation of tide level. It gradually varies during the long ebb tide., however, during the flood tide and the initial stage of the ebb tide, S_f varies more evidently in magnitude. In general, the main contribution of S_f comes from the slope of the water surface, $\partial h/\partial x$. The local acceleration term and the convective acceleration terms contribute much less in comparison to the gradient of the water surface for most of the time. Only during flood tide and the initial period of the ebb tide, do the acceleration terms increase significantly. The magnitude of the convective acceleration term is small compared to the gradient of water surface and the local acceleration term, with a small contribution only near the flood tide period.

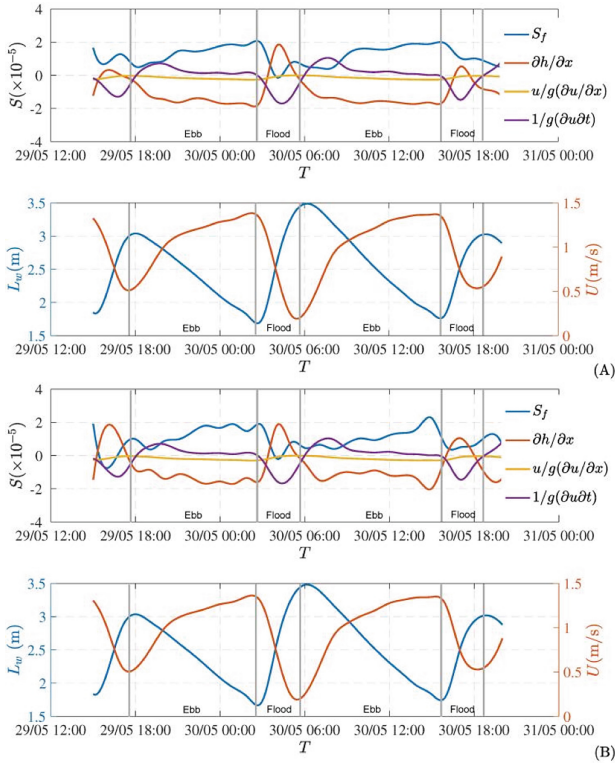


Fig. 2. Variation of different components of the energy slope during a complete tide cycle in the spring tide of a flood season. Plot (A) and (B) correspond to the DMA1 and DMA2 cross sections, respectively.

4.2 Variation of the Terms of Energy Slope in the Dry Season

Figure 3 shows the distribution of the magnitude of each term of the energy slope in a complete tidal cycle during the dry season. The gradient of water surface in DMA2 shows a more significant contribution to the total energy slope in comparison to the DMA1 which in combination with the weaker local acceleration terms in DMA2 makes the energy slope in DMA2 show a more gentle variation with time in comparison to that in DMA1. Compared to the flood season, the tidal magnitudes become smaller, decreasing from a tidal difference of around 2 m in the flood season to around 1 m in the dry season. In addition, the depth-averaged velocity also decreases from a range of 0.1 to 1.4 m/s during the flood season to 0.1 to 0.8 m/s during the dry season. The above variation decreases the magnitude of the items during the dry season. The trends shown in Fig. 3 are similar to the results in Fig. 2 to some extent, whereas differences can also be readily observed. The energy slope varies with the water level, and the main contribution comes from the water surface slope which is the same as the findings in the flood season. However, the relative contribution of local acceleration increases in comparison to the values in the flood season. During flood tide and initial ebb tide, the

magnitude of the local acceleration is comparable to that of the water surface slope, which causes a significant change in S_f . The decrease in the magnitude of each item makes the temporal change in S_f more significant and fluctuations more evident. Due to the vital influence of the water surface slope on the energy slope, it is supposed that the relation between the water level and the resistance coefficient will be improved in comparison to the widely used relation between resistance coefficient and flow depth.

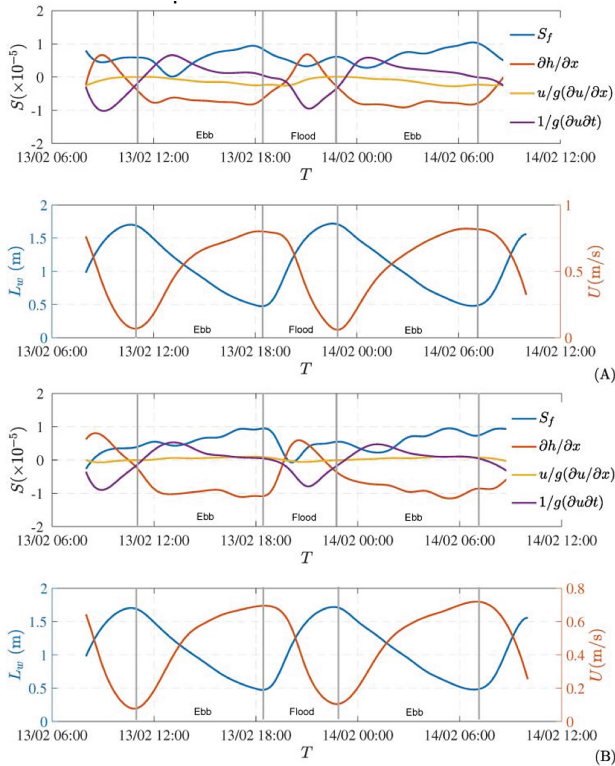


Fig. 3. Variation of different components of the energy slope during a complete tidal cycle in the spring tide of the dry season. Plot (A) and (B) correspond to the DMA1 and DMA2 cross-sections, respectively.

5 Discussion

In Knight (1981), local and convective accelerations were significant only when the water surface slope is around zero, and most of the time the energy slope consistently varies with the water surface slope. This differs to some extent from the results of this study. The contribution of local acceleration and convective acceleration terms to the energy slope compared to the water surface slope is much more evident than the results

found by Knight (1981). Although the results in this study show that the local and convective accelerations are certainly more significant when the water surface slope is zero, which is consistent with Knight's findings, their contributions remain significant throughout the flood tide and the initial ebb tide periods. This difference is mainly due to the fact that the magnitude of water surface variation in the straight section of the KW is smaller compared to the reach studied by Knight (1981); therefore, the change in water surface slope is less significant than that observed in Knight (1981). The KW is farther away from the Yangtse estuary (240 km) and thus has a smaller change in water surface gradient, compared to the Tal-y-Cafn reach studied by Knight (1981), which is only 10 km from the estuary. In addition, the Tal-y-Cafn section has a straight planar shape with little variation in cross-section along the course, while the cross-section morphology of the KW reach varies more evidently compared to the Tal-y-Cafn river, resulting in increased local and convective acceleration. These twofold impacts make the energy slope variation of the KW more complex than that observed by Knight (1981).

The effect of water depth on the resistance coefficient has been the major concern in river flow dynamics irrespective of tidal or non-tidal rivers. Many empirical formulas have been proposed to establish relations between water depth and flow coefficient (Yen 2002). A general form of such a relation can be obtained by combining the logarithmic equation of friction factor with the Manning equation. The logarithmic flow resistance for rough flow conditions is:

$$\frac{U}{u_*} = 6.25 + 5.75 \log_{10} \left(\frac{R}{k_s} \right) \quad (2)$$

where U and u_* are depth-averaged flow velocity and shear velocity, respectively. R is the hydraulic radius, and k_s is the roughness length scale. The Manning equation can be written as:

$$\frac{U}{u_*} = \frac{R^{1/6}}{n\sqrt{g}} \quad (3)$$

where n is the Manning coefficient and g is the gravity acceleration. Substitution of Eq. (2) into Eq. (3), the influence flow depth or hydraulic radius on the Manning coefficient can be obtained given a known k_s value:

$$n = \frac{\kappa R^{1/6}}{\sqrt{g} [\ln(R/k_s) - 1]} \quad (4)$$

where κ is the von Karman constant. This equation reflects the variation of flow resistance with hydraulic radius. Because the Manning coefficient varies with flow depth, mathematical models prefer to use Darcy-Weisbach factor to account for the flow resistance. However, it is difficult to accurately estimate k_s , because it changes with the variation of sediment transport conditions.

Figures 4 and 5 show the relations between Manning coefficient, n , with the water level, L_w , and hydraulic radius, R , respectively. The relation between n and L_w in Fig. 4 is much better than that between n and R . The most evident difference between them is that the n is uniformly distributed with the variation of the water level, i.e., the variance of the scattered points rarely changes with the varying water level. In contrast, the relation between n and the hydraulic radius shows an irregular distribution of the scattering points, that the variance of the points may increase or decrease with the varying hydraulic radius.

Equation (3) based on the logarithmic law was applied in Fig. 5 to compare with the measured data. Since the size of sand waves on the river bed is unknown, different k_s values from 0.05 to 0.2 m were applied to the equation. As shown in Fig. 5, the formula generally agrees with the measured data, but there is a significant deviation when the hydraulic radius is greater than 18 m. In addition, all the relations in Fig. 5 appear to be parallel straight lines, indicating that the formula predicts almost invariant Manning coefficients. However, as shown in Fig. 4, a trend of decreasing Manning coefficient as increasing water level can be readily observed. This is attributed to the fact that the shape of sand waves on the river bed changes with varying water levels, which further affects the resistance coefficient. Therefore, the relation between water level and resistance coefficient obtained based on the measured data is more suitable for the estimation of resistance coefficient in tidal rives in comparison to the relation based on the hydraulic radius. More importantly, there is no effective method to determine the k_s parameter, and thus the application of Eq. (3) is of great limitation. An empirical function was fitted between the Manning coefficient with the water level, and the correlation coefficient, R^2 , reaches 0.72, which can be used to estimate the resistance coefficient in the KW.

$$n = L_w^{-0.0047} \tag{5}$$

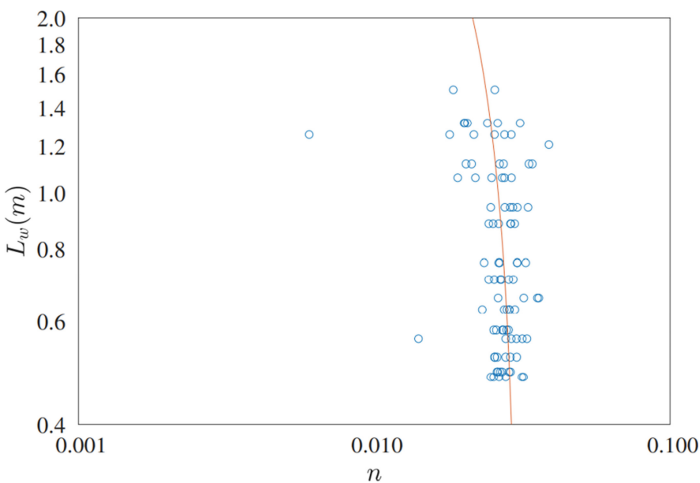


Fig. 4. Relation between water levels and the Manning coefficient

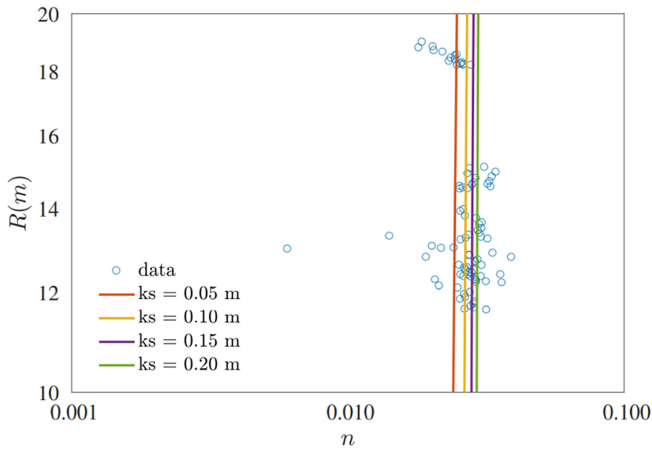


Fig. 5. Relation between the hydraulic radius and the Manning coefficient. The lines correspond to Eq. (4) with different k_s values.

6 Conclusions

By calculating the energy slope components of the KW during the flood and dry seasons, the contributions of different terms to the energy slope are compared during a complete tidal cycle. The following conclusions can be drawn from the results:

1. the water surface gradient is the main contribution to the energy slope irrespective of the flood or dry seasons.
2. the local acceleration and convective acceleration have a significant contribution to the total energy slope during the flood tide and initial stage of the ebb tide.
3. the relation between the resistance coefficient and the hydraulic radius during a complete tidal cycle is no better than the relation between the resistance coefficient and water levels. Therefore, in the lower reaches of the Yangtze River, the latter is preferred for estimating the resistance coefficient.
4. the coefficient of resistance varies in a limited range during tidal cycles, and thus applying a fixed Manning coefficient is an acceptable treatment if no prediction equation is available.

These results provide a reference for the resistance research in other tidal river reaches, whereas due to the empirical nature of the formula in this study, it is necessary to obtain a similar formula based on measured data.

Acknowledgements. This study was supported by the National Natural Science Foundation of China (52079043, 52179061).

References

- Bao W, Zhou J, Xiang X, Jiang P, Bao M (2018) A hydraulic friction model for one-dimensional unsteady channel flows with experimental demonstration. *Water* 10(1):43
- Brown WS, Richard PT (1980) A study of tidal energy dissipation and bottom stress in an estuary. *J Phys Oceanogr* 10(11):1742–1754
- Cao M, Li Q, Cai G, Yuan D, Wang X (2011) On local scour deformation flume generalization experiment of Manysha shoal head protection engineering in straight reach of Yangtze River estuary: I. Design of flume generalized and protection engineering building simulation. *Port WaterwEng* 7:106–112
- Hohermuth B, Weitbrecht V (2018) Influence of bed-load transport on flow resistance of step-pool channels. *Water Resour Res* 54(8):5567–5583
- Knight WD (1981) Some field measurements concerned with the behaviour of resistance coefficients in a tidal channel. *Estuar Coast Shelf Sci* 12(3):303–322
- Mrokowska MM, Rowiński PM, Kalinowska MB (2015) A methodological approach of estimating resistance to flow under unsteady flow conditions. *Hydrol Earth Syst Sci* 19:4041–4053
- Rowiński PM, Czernuszenko W, Marc J (2000) Time-dependent shear velocities in channel routing. *Hydrol Sci J* 45(6):881–895
- Rubol S, Ling B, Battiatto I (2018) Universal scaling-law for flow resistance over canopies with complex morphology. *Sci Rep* 8(1):1–15
- Pagliara S, Chiavaccini P (2006) Flow resistance of rock chutes with protruding boulders. *J Hydraul Eng* 132(6):545–552
- Yen BC (2002) Open channel flow resistance. *J Hydraul Eng* 128(1):20–39

Open Access This chapter is licensed under the terms of the Creative Commons Attribution 4.0 International License (<http://creativecommons.org/licenses/by/4.0/>), which permits use, sharing, adaptation, distribution and reproduction in any medium or format, as long as you give appropriate credit to the original author(s) and the source, provide a link to the Creative Commons license and indicate if changes were made.

The images or other third party material in this chapter are included in the chapter's Creative Commons license, unless indicated otherwise in a credit line to the material. If material is not included in the chapter's Creative Commons license and your intended use is not permitted by statutory regulation or exceeds the permitted use, you will need to obtain permission directly from the copyright holder.

